International Core Journal of Engineering Volume 11 Issue 4, 2025
ISSN: 2414-1895 DOI: 10.6919/ICJE.202504_11(4).0022

Formation Control of Unmanned Aerial Vehicles based on Cooperative Sliding Mode Adaptive Control

Minghui Xie[1], Hongwei Ren[2,*]

[1] College of Information and Control Engineering, Jilin Institute of Chemical Technology, Jilin, Jilin 132022, China

[2] College of Automation, Guangdong University of Petrochemical Technology, Maoming, Guangdong 525000, China

[*]Corresponding author: Hongwei Ren

Abstract

This paper investigates the formation control problem of quadrotor unmanned aerial vehicles (UAVs) under unknown disturbances and proposes a cooperative sliding mode adaptive control method to address the challenges of multi-UAV formation control in complex dynamic environments. To suppress the chattering phenomenon in sliding mode control, a saturation function is introduced, achieving smooth switching and effective suppression of high-frequency oscillations. The adaptive control mechanism dynamically adjusts control parameters based on real-time state errors, enhancing the system's robustness and adaptability. The cooperative control strategy ensures the synchronization and formation stability of multiple UAVs, successfully accomplishing the formation flight mission. The stability of the proposed strategy is proved using the Lyapunov method. Finally, using the leader-follower model, comparative simulations between cooperative sliding mode control and cooperative sliding mode adaptive control are conducted. The simulation results demonstrate that the proposed method has significant advantages in maintaining the desired formation, improving tracking accuracy, and enhancing disturbance rejection, providing an efficient and reliable solution for UAV formation control.

Keywords

Multi-UAV System; Formation Control; Cooperative Sliding Mode Adaptive Control.

1. Introduction

Formation control of Unmanned Aerial Vehicles remains a prominent research topic within the fields of control systems. Recent studies have particularly focused on the formation control of quadrotor UAVs, proposing various strategies to address the inherent challenges. For instance, Guo $et\ al.$ proposed an anti-disturbance formation control strategy for quadrotor UAVs, utilizing a disturbance observer to estimate and compensate for external disturbances [1]. Huang $et\ al.$ investigated finite-time formation tracking control with collision avoidance for multiple quadrotor UAVs, proving global stability using Lyapunov-like analysis [2]. Additionally, Guo $et\ al.$ presented a multiple observers-based anti-disturbance control scheme for quadrotor UAVs to combat model uncertainty and disturbance moments [3]. Li $et\ al.$ explored leader-follower formation control for multiple UAVs, addressing trajectory tracking issues through the implementation of virtual control variables [4]. In reference [5-[6]7], innovative strategies such as multi-constraint MPC, decentralized PID based on T-S fuzzy methods, distributed active disturbance rejection control, and fractional-order sliding surface adaptive control were utilized in quadrotor UAV formations. These approaches effectively

ISSN: 2414-1895 DOI: 10.6919/ICJE.202504_11(4).0022

addressed challenges such as external disturbances and communication constraints, significantly enhancing robustness, disturbance rejection, and trajectory tracking capabilities in complex environments. However, these improvements came at the cost of system responsiveness.

The literature on cooperative control of UAV formation has seen significant advancements recently. Wei *et al.* studied dynamic event-triggered cooperative formation control for UAVs subject to time-varying disturbances using a leader-follower framework [8]. Muslimov *et al.* introduced a consensus-based cooperative control approach for fixed-wing UAV formations [9], while Ma *et al.* focused on the impact of communication time delays on multi-UAV cooperative formation control [10]. While multi-UAV formation collaborative control offers advantages such as improved task efficiency and flexibility, it also faces challenges including difficult communication coordination, Relatively poor disturbance rejection capability, and slow response speeds.

Particularly in the application of cooperative sliding mode control, recent research has shown considerable interest. Tahir *et al.* proposed a multi-layered and distributed control system for a swarm of drones in a hierarchical formation based on the leader-follower approach, aiming to reduce the complexity of developing large systems [11]. In reference [12-13], formation control was achieved using backstepping cooperative techniques and a distributed sliding mode control protocol with time-varying tracking, enabling rapid formation and excellent tracking performance for multiple UAVs. Yuan *et al.* introduced a data-driven model-free adaptive control method for quadrotor formation trajectory that enhances dynamic response and accuracy [14].

To enhance the disturbance rejection capabilities, response speed, and formation control ability of multi-UAV systems, a UAV formation control method based on cooperative sliding mode adaptive control has been proposed. The innovations are as follows:

1) By leveraging strong robustness, real-time adaptive adjustment, and multi-UAV coordination, the method achieves simplified design, high-precision tracking, and strong disturbance rejection, making it particularly suitable for UAV formation control in complex dynamic environments.

2) Simulations under identical conditions are conducted for both cooperative sliding mode control and cooperative sliding mode adaptive control. The performance of these two control methods is compared by analyzing the consistency of position states and velocity states.

3) By smoothing control inputs, reducing high-frequency switching, minimizing discontinuities, and protecting actuators, the saturation matrix function effectively suppresses chattering in sliding mode control.

The structure of this brief is as follows. In Section II, the relevant theorems and graph theory fundamentals are described. In Section III, the problem statement is provided, clarifying the research subject and objectives. In Section IV, a cooperative sliding mode adaptive control strategy is proposed, detailing the algorithm design and implementation process. The effectiveness and advantages of the proposed strategy are verified through comparative simulations in Section V. Finally, in Section VI, the research is summarized.

2. Preliminaries

Given a matrix X, X^T denotes its transpose. $X > 0 (< 0)$ indicates that X is a symmetric positive (negative) definite matrix. The set $\mathbb{R}^n$ represents the real numbers. The symbol $\otimes$ denotes the Kronecker product.

Lemma 1: For real matrices A, B, C, and D with appropriate dimensions, the Kronecker product $\otimes$ has the following properties [15]:

1) $(A+B)\otimes C = A\otimes C + B\otimes C$,

2) $(A\otimes B)^T = A^T + B^T$,

3) $(A\otimes B)(C\otimes D) = (AC)\otimes(BD)$.

ISSN: 2414-1895 DOI: 10.6919/ICJE.202504_11(4).0022

Lemma 2: Let A be an $n\times m$ matrix with elements a_{ij}. The saturation function restricts each element to the range $[-1,1]$.

$$\text{sat}(A)=\begin{bmatrix}\text{sat}(a_{11}) & \text{sat}(a_{12}) & \cdots & \text{sat}(a_{1m})\\ \text{sat}(a_{21}) & \text{sat}(a_{22}) & \cdots & \text{sat}(a_{2m})\\ \vdots & \vdots & \ddots & \vdots\\ \text{sat}(a_{n1}) & \text{sat}(a_{n2}) & \cdots & \text{sat}(a_{nm})\end{bmatrix}$$

The expression of the saturation function is

$$sat(a_{ij})=\begin{cases}1 & , \quad a_{ij}\geq 1\\ -1 & , \quad a_{ij}\leq -1\end{cases}$$

Lemma 3 (Young's Inequality): For any non-negative real numbers a and b, and positive real numbers p and q satisfying $p^{-1}+q^{-1}=1$, the following inequality holds [16]:

$$ab\leq p^{-1}a^{p}+q^{-1}b^{q}$$

where equality is achieved if and only if $a^{p}=b^{q}$.

A directed graph $G=(V,E)$ consists of a set of vertices $V=\{v_1,v_2,\cdots,v_n\}$ and a set of directed edges $E\subseteq V\times V$. The adjacency matrix A of a directed graph is an $n\times n$ matrix, where a_{ij} represents the existence and weight of an edge from vertex v_i to vertex v_j. If there is an edge (v_i,v_j), then $a_{ij}\neq 0$; otherwise, $a_{ij}=0$. The degree matrix D is a diagonal matrix, where the diagonal element d_{ii} represents the number or sum of weights of edges originating from vertex v_i. The Laplacian matrix L is defined as $L=D-A$.

3. Problem Statement

The relationship between the control inputs of a quadrotor UAV and the squared rotor speeds is as follows:

$$\begin{bmatrix}u_{i1}\\ u_{i2}\\ u_{i3}\\ u_{i4}\end{bmatrix}=\begin{bmatrix}\rho & \rho & \rho & \rho\\ 0 & -l\rho & 0 & l\rho\\ -l\rho & 0 & l\rho & 0\\ d & d & d & d\end{bmatrix}\begin{bmatrix}\omega_{i1}^{2}\\ \omega_{i2}^{2}\\ \omega_{i3}^{2}\\ \omega_{i4}^{2}\end{bmatrix} \tag{1}$$

In the matrix, ρ is the thrust coefficient, l is the arm length, and d is the drag coefficient.

The classic quadcopter UAV model is

$$\begin{aligned}J_{ix}\ddot{\varphi}_i &= (J_{iy}-J_{iz})\dot{\theta}_i\dot{\psi}_i+u_{i2}-J_{ir}\dot{\theta}_i\omega_{ir}\\ J_{iy}\ddot{\theta}_i &= (J_{iz}-J_{ix})\dot{\varphi}_i\dot{\psi}_i+u_{i3}-J_{ir}\dot{\varphi}_i\omega_{ir}\\ J_{iz}\ddot{\psi}_i &= (J_{ix}-J_{iy})\dot{\theta}_i\dot{\varphi}_i+u_{i4}\end{aligned} \tag{2}$$

ISSN: 2414-1895 DOI: 10.6919/ICJE.202504_11(4).0022

In the dynamics of an aircraft, J_{ix}, J_{iy}, and J_{iz} represent the principal components of the inertia matrix. φ_i, θ_i, and ψ_i denote the pitch, roll, and yaw angles of the UAV, respectively. $\dot{\varphi}_i$, $\dot{\theta}_i$, and $\dot{\psi}_i$ represent the corresponding angular velocities. $\ddot{\varphi}_i$, $\ddot{\theta}_i$, and $\ddot{\psi}_i$ denote the angular accelerations about the X, Y, and Z axes, respectively. u_{i2}, u_{i3}, and u_{i4} are the control inputs for the X, Y, and Z axes. J_{ir} represents the inertia of the UAV's rotor, and ω_{ir} denotes the rotor's rotational speed.

$$\ddot{p}_i = \frac{u_{i1}}{m} R_b^e e_3 - g e_3 \tag{3}$$

Where $p_i = \begin{bmatrix} p_{ix} & p_{iy} & p_{iz} \end{bmatrix}^T$ represents the position states of the UAV along the X, Y, and Z axes, u_{i1} is the total thrust, m is the mass, R_b^e is the rotation matrix converting from the UAV body frame to the inertial frame, e_3 is the unit vector $[0,0,1]^T$, and g is the gravitational acceleration.

The expression for the rotating coordinate system is as follows [17]:

$$R_b^e = R(\theta)R(\varphi)R(\psi) \tag{4}$$

Where $R(\theta)$, $R(\varphi)$, and $R(\psi)$ represent the rotation matrices for the three angles. The expression is as follows:

$$R(\theta) = \begin{bmatrix} \cos(\theta) & 0 & -\sin(\theta) \\ 0 & 1 & 0 \\ \sin(\theta) & 0 & \cos(\theta) \end{bmatrix} R(\varphi) = \begin{bmatrix} 1 & 0 & 0 \\ 0 & \cos(\varphi) & \sin(\varphi) \\ 0 & -\sin(\varphi) & \cos(\varphi) \end{bmatrix} R(\psi) = \begin{bmatrix} \cos(\psi) & \sin(\psi) & 0 \\ -\sin(\psi) & \cos(\psi) & 0 \\ 0 & 0 & 1 \end{bmatrix} \tag{5}$$

Assumption 1: Assume that the disturbance $d(t)$ is unknown but bounded by known.

Assumption 2: The topology structure G is strongly connected, ensuring that each UAV is linked to the leader node through at least one stable communication path.

A UAV can be represented as a double integrator multi-agent system, where the system manipulates the position of each UAV. Considering a scenario with one leader UAV and N follower UAVs, all characterized by the same non-linear dynamics, the mathematical model is as follows:

$$\begin{aligned} \dot{P}_i(t) &= V_i(t) \\ \dot{V}_i(t) &= U_i(t) \end{aligned} \tag{6}$$

Where $P_i(t)$, $V_i(t)$, and $U_i(t)$ are vectors in $\mathbb{R}^n$. Additionally, $P_i(t)$ represents the position of the UAV, $V_i(t)$ represents the velocity of the UAV, and $U_i(t)$ represents the control input of the UAV. The dynamic model of the leader UAV is as follows:

$$\begin{aligned} \dot{P}_r(t) &= V_r(t) \\ \dot{V}_r(t) &= U_r(t) \end{aligned} \tag{7}$$

ISSN: 2414-1895 DOI: 10.6919/ICJE.202504_11(4).0022

The $U_i(t)$ contains two inputs, one is the controller input, and the other part is the external bounded disturbance input. $U_i(t) = u_i(t) + d_i(t)$. Where $d_i(t) = \left[d_{ix}(t) \quad d_{iy}(t) \quad d_{iz}(t) \right]^T$. The synchronization error between the i-th UAV and the leader UAV is defined as

$$\begin{aligned} \delta_{ip}(t) &= P_i(t) - P_r(t) \\ \delta_{iv}(t) &= V_i(t) - V_r(t) \end{aligned} \tag{8}$$

Theorem 1: For a group of UAVs $i = 1, 2, \ldots, N$, if the following conditions are satisfied as time t approaches infinity.

$$\begin{aligned} &\lim_{t\to\infty} \| P_i(t) - P_r(t) \| \to 0 \\ &\lim_{t\to\infty} \| V_i(t) - V_r(t) \| \to 0 \end{aligned} \tag{9}$$

Then the UAV formation is said to have achieved consensus, even in the presence of nonlinear errors $d_i(t)$. This also indicates the realization of unified action and stable configuration throughout the formation.

4. Collaborative Sliding Mode Adaptive Controller Design

The collaborative sliding mode adaptive controller, as a composite control strategy, combines the advantages of sliding mode control and adaptive control to improve the performance and robustness of the system. Its core design consists of two parts: the sliding mode part and the adaptive part. The former achieves rapid stabilization of the system state through sliding surfaces and sliding control laws, while the latter estimates and adjusts the unknown parameters of the system in real time through parameter estimators and parameter adjustment laws to cope with changes in system dynamics and parameter uncertainties. This controller design considers the dynamic characteristics of the system, nonlinear factors, and external disturbances, while also addressing issues of real-time performance and computational complexity. It is capable of stable and reliable operation under conditions of bounded disturbances.

To enhance clarity, reduce formula complexity and ambiguity, and adhere to mathematical conventions, the function $s_i(t)$ will be represented as s_i . Similarly, other instances will follow the same convention.

In traditional formation control, the standard cooperative controller output u_i is given by [18]:

$$u_i(t) = -\alpha(p_i(t) - p_i^* + \gamma(v_i(t) - v_i^*) - \beta\sum_i^N a_{ij}\left[\ (p_i(t) - p_i^*) - (p_j(t) - p_j^*) + \gamma\left((v_i(t) - v_i^*) - (v_j(t) - v_j^*)\right) \ \right] \tag{10}$$

The gain coefficients α, β, and γ are positive constants. This approach ensures good performance in terms of coherence and tracking, especially in scenarios involving multiple UAVs working cooperatively. However, if there are unmodeled dynamics or external disturbances in the system, the control performance may be significantly affected.

Due to its inherent robustness, sliding mode control exhibits strong suppression capabilities against system parameter variations and external disturbances. The saturation function $sat(t)$ further enhances control over oscillations, making it perform better in complex and varying environments. In sliding mode control, the sliding surface is selected as:

ISSN: 2414-1895 DOI: 10.6919/ICJE.202504_11(4).0022

$$s_i = \delta_{ip} - P_i^* + \gamma\delta_{iv} \tag{11}$$

Here, The parameter γ is a tuning parameter. The fixed offset P_i^* ensures that each follower UAV in the formation maintains a constant relative position with respect to the leader and other UAVs, thereby preserving the formation shape and stability. Even if the position of the leader changes, the follower UAVs can adjust their positions based on P_i^* to maintain coordinated formation.

$$U_i = -\gamma^{-1}\left(\alpha \otimes s_i + \beta L \otimes s_i + \lambda sat(s_i) + \delta_{iv} + d_i\right) \tag{12}$$

Proof 1: Considering equations (6) and (12), and differentiating the sliding surface s_i with respect to time according to equation (11), we obtain:

$$\dot{s}_i = \delta_{iv} + \gamma(\dot{V}_i - \dot{V}_r) \tag{13}$$

Let's choose the Lyapunov function $V_1(s) = \frac{1}{2}s_i^T s_i$, and then find its derivative as follows:

$$\begin{aligned}
\dot{V}_1(s) &= s_i^T \dot{s}_i = s_i^T(\delta_{iv} + \gamma(\dot{V}_i - \dot{V}_r)) \\
&= s_i^T\left(\delta_{iv} - \gamma\left(\alpha \otimes s_i + \beta L \otimes s_i + \lambda \text{sat}(s_i) + \delta_{iv} + d_i\right)\right) \\
&= -s_i^T\left(\alpha \otimes s_i + \beta L s_i + \lambda \text{sat}(s_i) + \gamma d_i\right) \\
&= -\left(\alpha \otimes I_N + \beta L\right) \otimes s_i^T s_i - \lambda|s_i| - \gamma d_i
\end{aligned} \tag{14}$$

We can observe that $\dot{V}_1(s)$ is a negative semi-definite function because α, β, λ, γ are all positive, and $s_i^T s_i \geq 0$. This indicates that the system is stable under the Lyapunov function $V_1(s)$.

Compared to cooperative sliding mode control, adding adaptive control to the code offers significant advantages in multi-UAV formation control. The adaptive control strategy enhances system robustness, adapts to unknown system dynamics and external disturbances, reduces the need for parameter tuning, improves tracking performance and stability, and is more suitable for complex and changing environments.

$$U_i(t) = -\gamma^{-1}\left(\alpha \otimes s_i + \beta L \otimes s_i + \lambda sat(s_i) + \delta_{iv} + d_i\right) + \gamma\hat{\vartheta} \otimes d_i \tag{15}$$

Where ϑ represents the true parameters of the system. $\hat{\vartheta}$ is the estimated value of the system parameters, and $\tilde{\vartheta}$ is the difference between the true parameters and their estimated values.

where $\tilde{\vartheta}_i = \hat{\vartheta}_i - \vartheta_i$ denotes the parameter estimation error.

Selecting the adaptive rate as follows:

$$\dot{\hat{\vartheta}}_i = -\gamma s_i \otimes d_i - c\hat{\vartheta}_i \tag{16}$$

Proof 2: We consider the Lyapunov function candidate $V(s_i, \tilde{\vartheta}_i)$:

ISSN: 2414-1895 DOI: 10.6919/ICJE.202504_11(4).0022

$$V(s_i, \vartheta_i) = \frac{1}{2} s_i^T s_i + \frac{1}{2} \tilde{\vartheta}_i^T \tilde{\vartheta}_i \tag{17}$$

Differentiating V with respect to time gives:

$$\dot{V}(s_i, \tilde{\vartheta}_i) = s_i^T \dot{s}_i + \tilde{\vartheta}_i^T \dot{\tilde{\vartheta}}_i \tag{18}$$

Substituting the expressions for (13) and (16), we obtain:

$$\begin{aligned} \dot{V}(s_i, \tilde{\vartheta}_i) &= s_i^T (V_i + \gamma \dot{V}_i) + \widetilde{\vartheta}_i^T \dot{\hat{\vartheta}}_i \\ &= s_i^T \left(V_i - \left(\alpha \otimes s_i + \beta L \otimes s_i + \lambda sat(s_i) + V_i \right) - \gamma \vartheta_i^T \otimes d_i + \gamma \hat{\vartheta}_i^T \otimes d_i \right) + \widetilde{\vartheta}_i^T \dot{\hat{\vartheta}}_i \\ &= -\left(\alpha I_N + \beta L \right) \otimes s_i^T s_i - \lambda \left| s_i \right| + \tilde{\vartheta}_i^T (\gamma \otimes s_i^T d + \dot{\hat{\vartheta}}_i) \\ &= -(\alpha \otimes I_N + \beta L) \otimes s_i^T s_i - \lambda \mid s_i \mid - c \tilde{\vartheta}_i^T \hat{\vartheta}_i \\ &= -(\alpha \otimes I_N + \beta L) \otimes s_i^T s_i - \lambda \mid s_i \mid - c \tilde{\vartheta}_i^T \tilde{\vartheta}_i - c \tilde{\vartheta}_i^T \vartheta_i \end{aligned} \tag{19}$$

By applying the Lemma 3, the cross-term $\tilde{\vartheta}_i^T \vartheta_i$ can be bounded by:

$$\tilde{\vartheta}_i^T \vartheta_i \le \frac{c}{2} \tilde{\vartheta}_i^T \tilde{\vartheta}_i + \frac{c}{2} \vartheta_i^T \vartheta_i \tag{20}$$

Thus, $\dot{V}$ simplifies to:

$$\dot{V}(s_i, \tilde{\vartheta}_i) \le \ -(\alpha \otimes I_N + \beta L) \otimes s_i^T s_i - \lambda \mid s_i \mid - \frac{c}{2} \tilde{\vartheta}_i^T \tilde{\vartheta}_i + \frac{c}{2} \vartheta_i^T \vartheta_i \tag{21}$$

Since the terms involving s_i and $\tilde{\vartheta}_i$ are negative definite and semi-definite respectively, and ϑ_i is bounded, it ensures the stability of the sliding mode and convergence of the parameter estimation error $\tilde{\vartheta}_i$ towards zero.

5. Simulation of UAV Formation Control under Bounded Disturbances

In this section, we validate the effectiveness of the proposed scheme through simulation experiments. The experiment involves one UAV acting as the leader (denoted as UAV 1) and four UAVs acting as followers (denoted as UAVs 2 to 5). The task of these UAVs is to fly in a linear formation and follow the leader's trajectory according to the predetermined formation mission.

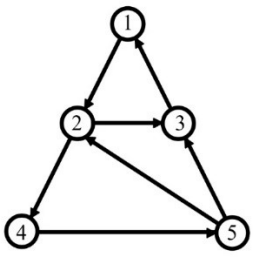

Fig. 1 The network communication topology among drones.

ISSN: 2414-1895 DOI: 10.6919/ICJE.202504_11(4).0022

Table 1. The desired final shape, initial position, and initial velocity of each UAV.

Desired positions	Initial position	Initial velocity
$h_1 = [0,0,0]^T$	$P_1(0) = [-25,9,150]^T$	$V_1(0) = [20,10,10]^T$
$h_2 = [20,0,0]^T$	$P_2(0) = [-70,-1.2,140]^T$	$V_2(0) = [20,9,11]^T$
$h_3 = [40,0,0]^T$	$P_3(0) = [-50,4,100]^T$	$V_3(0) = [20,12,10]^T$
$h_4 = [60,0,0]^T$	$P_4(0) = [-20,1,160]^T$	$V_4(0) = [20,10,10]^T$ \$
$h_5 = [80,0,0]^T$	$P_5(0) = [-10,10,175]^T$	$V_5(0) = [20,8,10]^T$

From the communication topology diagram in Fig. 1, the Laplacian matrix of the system can be obtained as follows:

$$L = \begin{bmatrix} 1 & -1 & 0 & 0 & 0 \\ 0 & 2 & -1 & -1 & 0 \\ -1 & 0 & 1 & 0 & 0 \\ 0 & 0 & 0 & 1 & -1 \\ 0 & -1 & -1 & 0 & 2 \end{bmatrix}$$

Taking into account the external bounded interference proposed in reference [19], assume:

$$d_i(t) = [10\sin(1.5t(k));10\sin(1.5t(k));10\sin(1.5t(k))]$$

In this study, we conducted two sets of simulation experiments. In Simulation 1, the controller used was the cooperative sliding mode control, while in Simulation 2, the cooperative sliding mode adaptive control was employed. In both simulations, we used the same bounded disturbances and communication protocol to ensure consistency in experimental conditions. By comparing the performance of these two control strategies under identical conditions, we can evaluate the effectiveness of the adaptive mechanism in handling disturbances and enhancing system performance.

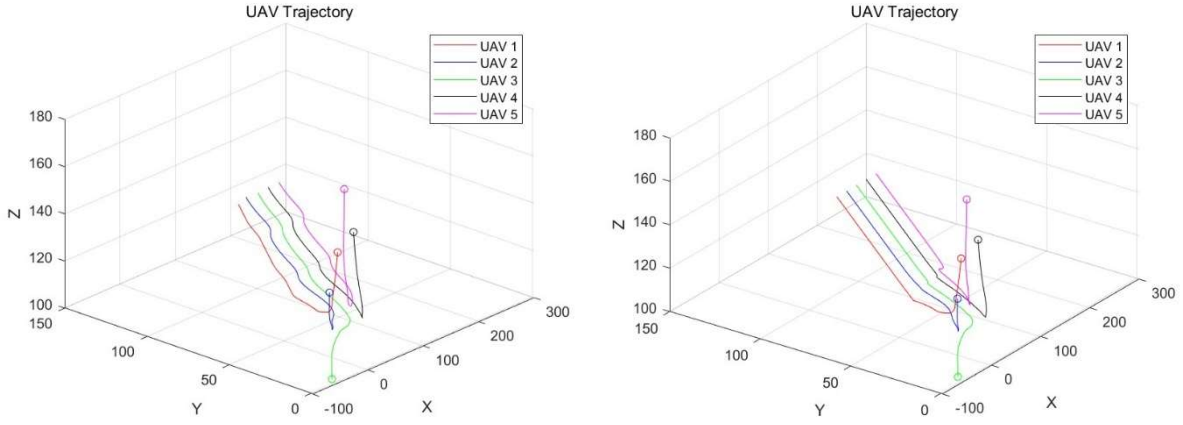

(a) (b)

Fig. 2 Trajectory of five UAVs in 3D space: (a) Cooperative Sliding Mode Control, (b) Cooperative Sliding Mode Adaptive control

ISSN: 2414-1895 DOI: 10.6919/ICJE.202504_11(4).0022

In Fig. 2, the trajectories of the five UAVs are plotted to demonstrate the differences in the final simulated shape throughout the simulation. Fig. 2(a) shows the trajectory using cooperative sliding mode control, where significant nonlinearities in the trajectories are evident due to disturbances. Under the same disturbance and communication conditions, the UAV trajectories with cooperative sliding mode adaptive control are smoother, converge faster, and better achieve the desired formation shape.

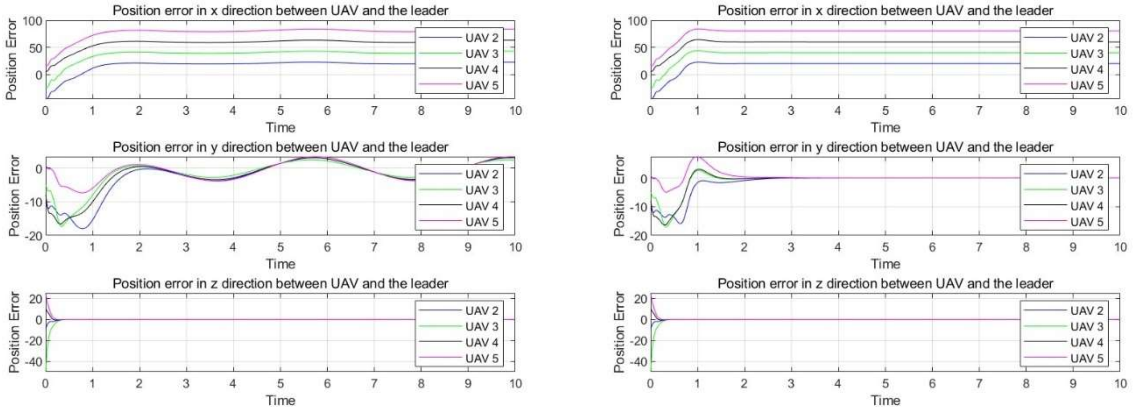

(a) (b)

Fig. 3 Position error between UAVs and the leader in X, Y, and Z directions: (a) Cooperative Sliding Mode Control, (b) Cooperative Sliding Mode Adaptive control

Fig. 3 illustrate the position errors between the UAVs and the leader under two different simulation conditions. Each UAV maintains the same distance on the X-axis, with a fixed spacing $D = 20$ between adjacent UAVs. Fig. 3 (a) shows the position error under cooperative sliding mode control, which has higher residual errors and slower convergence speed. In contrast, Fig. 3 (b) displays the position errors under cooperative sliding mode adaptive control, demonstrating significant advantages in dealing with bounded disturbances and communication conditions. Specifically, the position errors converge faster and have smaller residual errors, with superior convergence characteristics in the x, y, and z directions, the position errors exhibit superior convergence characteristics, achieving the desired positions.

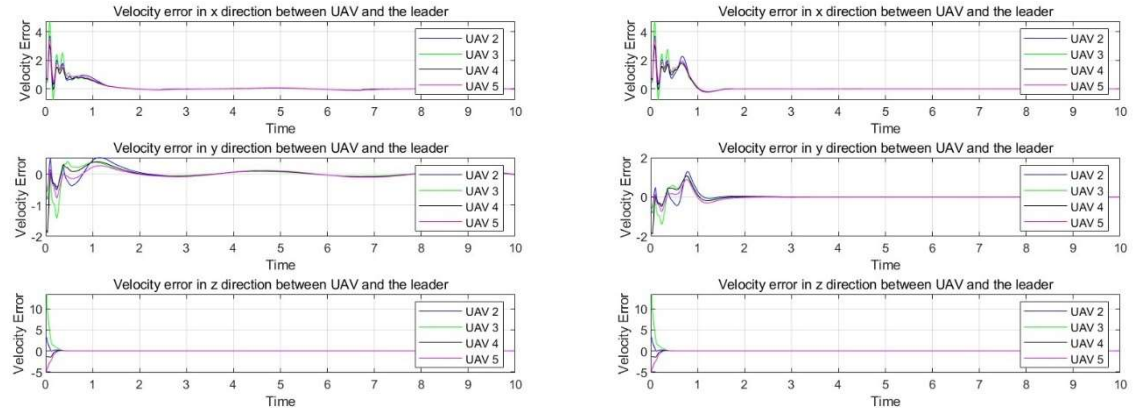

(a) (b)

Fig. 4 Velocity error between UAVs and the leader in X, Y, and Z directions: (a) Cooperative Sliding Mode Control, (b) Cooperative Sliding Mode Adaptive control

ISSN: 2414-1895 DOI: 10.6919/ICJE.202504_11(4).0022

Fig. 4 illustrate the velocity errors between the UAVs and the leader. Fig. 4 (a) shows the velocity error under cooperative sliding mode control, where initial fluctuations are large, convergence speed is slow, and residual errors are high. In contrast, Fig. 4 (b) displays the velocity error under cooperative sliding mode adaptive control. This method exhibits faster convergence speed and lower residual errors, with superior convergence characteristics in the x, y, and z directions.

Through simulation comparisons of the two control methods, cooperative sliding mode adaptive control demonstrated significant advantages in handling bounded disturbances when observed from the formation's position and velocity states. It effectively enhanced the system's accuracy and robustness while ensuring rapid responsiveness.

6. Conclusion

In this study, we compared the performance of cooperative sliding mode control and cooperative sliding mode adaptive control in multi-UAVs systems through simulation experiments. The experimental results indicate that cooperative sliding mode adaptive control exhibits significant advantages under bounded disturbances and communication conditions, demonstrating faster convergence speed and lower residual errors, particularly in position and velocity error convergence characteristics. This provides important theoretical support and experimental evidence for optimizing control strategies in multi-UAVs systems.

References

[1] Kexin Guo, Cai Liu, Xiao Zhang, Xiang Yu, Lei Guo, and Youmin Zhang. Disturbance perception based quadrotor uav maneuvering formation against unknown external disturbance. In 2020 International Conference on Unmanned Aircraft Systems (ICUAS), pages 117–122. IEEE, 2020.

[2] Youfang Huang, Wen Liu, Bo Li, Yongsheng Yang, and Bing Xiao. Finite-time formation tracking control with collision avoidance for quadrotor uavs. Journal of the Franklin Institute, 357(7):4034–4058, 2020.

[3] Kexin Guo, Jindou Jia, Xiang Yu, Lei Guo, and Lihua Xie. Multiple observers based anti-disturbance control for a quadrotor uav against payload and wind disturbances. Control Engineering Practice, 102:104560, 2020.

[4] Hang Li, Jing Wang, Cunwu Han, Meng Zhou, and Zhe Dong. Leaderfollower formation control of mutilple uavs based on adrc: experiment research. In 2021 4th IEEE International Conference on Industrial Cyber-Physical Systems (ICPS), pages 558–565. IEEE, 2021.

[5] Bor-Sen Chen, Yi-Chen Liu, Min-Yen Lee, and Chih-Lyang Hwang. Decentralized h pid team formation tracking control of large-scale quadrotor uavs under external disturbance and vortex coupling. IEEE Access, 10:108169–108184, 2022.

[6] Danghui Yan, Weiguo Zhang, Hang Chen, and Jingping Shi. Robust control strategy for multi-uavs system using mpc combined with kalmanconsensus filter and disturbance observer. ISA transactions, 135:35–51, 2023.

[7] Hongbin Wang, Ning Li, and Qianda Luo. Adaptive fractional-order nonsingular fast terminal sliding mode formation control of multiple quadrotor uavs-based distributed estimator. Asian Journal of Control, 25(5):3671–3686, 2023.

[8] Lili Wei, Mou Chen, and Tao Li. Dynamic event-triggered cooperative formation control for uavs subject to time-varying disturbances. IET Control Theory & Applications, 14(17):2514–2525, 2020.

[9] Tagir Z Muslimov and Rustem A Munasypov. Consensus-based cooperative control of parallel fixed-wing uav formations via adaptive backstepping. Aerospace science and technology, 109:106416, 2021.

[10] Peibei Ma, Jun Ji, Jiangbo Sui, and Ming Lei. Research on cooperative formation flight control of multi-uav with communication time delay. In 2021 International Conference on Control Science and Electric Power Systems (CSEPS), pages 54–58. IEEE, 2021.

[11] Anam Tahir, Jari M Boling, Mohammad-Hashem Haghbayan, and Juha ¨Plosila. Comparison of linear and nonlinear methods for distributedcontrol of a hierarchical formation of uavs. IEEE Access, 8:95667–95680, 2020.

ISSN: 2414-1895 DOI: 10.6919/ICJE.202504_11(4).0022

[12] Jialong Zhang, Jianguo Yan, and Pu Zhang. Multi-uav formation control based on a novel back-stepping approach. IEEE Transactions on Vehicular Technology, 69(3):2437–2448, 2020.

[13] Jianhua Wang, Liang Han, Xiwang Dong, Qingdong Li, and Zhang Ren. Distributed sliding mode control for time-varying formation tracking of multi-uav system with a dynamic leader. Aerospace Science and Technology, 111:106549, 2021.

[14] Dongdong Yuan and Yankai Wang. Data driven model-free adaptive control method for quadrotor formation trajectory tracking based on rise and ismc algorithm. Sensors, 21(4):1289, 2021.

[15] Juan A Vazquez Trejo, Damiano Rotondo, Manuel Adam Medina, and Didier Theilliol. Robust observer-based leader-following consensus for a class of nonlinear multi-agent systems: application to uav formation control. In 2021 International Conference on Unmanned Aircraft Systems (ICUAS), pages 1565–1572. IEEE, 2021.

[16] Herm Jan Brascamp and Elliott H Lieb. Best constants in young's inequality, its converse, and its generalization to more than three functions. Advances in Mathematics, 20(2):151–173, 1976.

[17] Liqian Dou, Siyuan Cai, Xiuyun Zhang, Xiaotong Su, and Ruilong Zhang. Event-triggered-based adaptive dynamic programming for distributed formation control of multi-uav. Journal of the Franklin Institute, 359(8):3671–3691, 2022.

[18] Zhang Ren, Mengyi Wang, and Yongzhao Hua. Proceedings of 2021 5th Chinese Conference on Swarm Intelligence and Cooperative Control. Springer, 2023.

[19] Xue-ying Jiang, Cheng-li Su, Ya-peng Xu, Kai Liu, Hui-yuan Shi, and Ping Li. An adaptive backstepping sliding mode method for flight attitude of quadrotor uavs. Journal of Central South University, 25(3):616–631, 2018.